The Company of
Biologists

RESEARCH ARTICLE

Scaling of fibre area and fibre glycogen concentration in the hindlimb musculature of monitor lizards: implications for locomotor performance with increasing body size

Robert L. Cieri[1,*], Taylor J. M. Dick[1,2], Jeremy S. Morris[3] and Christofer J. Clemente[1,2]

ABSTRACT

A considerable biomechanical challenge faces larger terrestrial animals as the demands of body support scale with body mass (M_b), while muscle force capacity is proportional to muscle cross-sectional area, which scales with $M_b^{2/3}$. How muscles adjust to this challenge might be best understood by examining varanids, which vary by five orders of magnitude in size without substantial changes in posture or body proportions. Muscle mass, fascicle length and physiological cross-sectional area all scale with positive allometry, but it remains unclear, however, how muscles become larger in this clade. Do larger varanids have more muscle fibres, or does individual fibre cross-sectional area (fCSA) increase? It is also unknown if larger animals compensate by increasing the proportion of fast-twitch (higher glycogen concentration) fibres, which can produce higher force per unit area than slow-twitch fibres. We investigated muscle fibre area and glycogen concentration in hindlimb muscles from varanids ranging from 105 g to 40,000 g. We found that fCSA increased with modest positive scaling against body mass ($M_b^{0.197}$) among all our samples, and $\propto M_b^{0.278}$ among a subset of our data consisting of never-frozen samples only. The proportion of low-glycogen fibres decreased significantly in some muscles but not others. We compared our results with the scaling of fCSA in different groups. Considering species means, fCSA scaled more steeply in invertebrates ($\propto M_b^{0.575}$), fish ($\propto M_b^{0.347}$) and other reptiles ($\propto M_b^{0.308}$) compared with varanids ($\propto M_b^{0.267}$), which had a slightly higher scaling exponent than birds ($\propto M_b^{0.134}$) and mammals ($\propto M_b^{0.122}$). This suggests that, while fCSA generally increases with body size, the extent of this scaling is taxon specific, and may relate to broad differences in locomotor function, metabolism and habitat between different clades.

KEY WORDS: Fibre type, Muscle architecture, Scaling, Varanids, Reptiles, Musculoskeletal system

INTRODUCTION

Any factor that limits muscle force production is destined to contribute to limits on animal locomotor performance. The maximum force-generating capacity and maximum contraction speed of a muscle are important factors in determining how forcefully and quickly animals can move their limbs, ultimately limiting speed, manoeuvrability and locomotor performance (Biewener, 2005; Biewener and Patek, 2018). These limits become even more critical as animals increase in size because a muscle's force production capacity depends on cross-sectional area, which increases at a lower rate than body mass ($\propto M_b^{2/3}$) (Dick and Clemente, 2017). Among geometrically similar animals, this biomechanical challenge suggests that larger animals will be proportionally weaker than smaller animals. As a result, larger animals compensate with allometric shifts in limb posture or musculoskeletal architecture and suffer reduced maximum sprint speed and increased duty factor (Cieri et al., 2021; Clemente et al., 2013; Dick and Clemente, 2017). For example, many mammals compensate for predicted decreases in proportional strength by adopting a more erect posture, thereby increasing the effective mechanical advantage of the extensor muscles and allowing animals to locomote effectively without substantial changes in muscle architecture (Biewener, 1989, 2005).

In varanid lizards, however, where posture does not vary across a substantial body size range (Clemente et al., 2011), allometric increases in muscle mass, physiological cross-sectional area (PCSA) and fascicle length occur in many hindlimb and forelimb muscles (Cieri et al., 2020; Dick and Clemente, 2016). Similar trends are displayed in felids, another tetrapod group that also maintain a crouched posture even at larger body sizes, however the allometry is less pronounced than varanids and is not significant when accounting for phylogeny (Cuff et al., 2016a,b). Sprawling locomotion was widespread in stem tetrapods, thus allometric increases in muscle size were likely important for the locomotion of larger animals even before the rise of animals with parasagittal gaits (Dick and Clemente, 2017).

Increased PCSA in the muscles of larger species can be accomplished either by larger animals simply having more muscle fibres in parallel (increasing fibre number, hyperplasia) or by increasing the cross-sectional area of individual muscle fibres (fCSA, hypertrophy). The fibres themselves can also vary in biochemistry. Larger muscle fibres, which typically are more glycolytic, have a higher tension cost (ATP required to generate tension) than smaller fibres, which tend to be oxidative (Bottinelli et al., 1994; Rome and Lindstedt, 1997). The small fCSA of slow oxidative fibres facilitates timely oxygen diffusion that is necessary for aerobic metabolism (Hardy et al., 2009; Kinsey et al., 2011; Van Wessel et al., 2010). By contrast, fibres with larger fCSA generally power muscle activity via glycolytic metabolism and are capable of generating larger forces because a greater proportion of their internal area is occupied by contractile myofilaments (reviewed in Schiaffino and Reggiani, 2011). Fast-twitch muscles, which use glycolytic metabolism, are often associated with anaerobic sprinting in lizards (Bonine et al., 2005; Jayne et al., 1990), suggesting that

[1]School of Science and Engineering, University of the Sunshine Coast, Sippy Downs, QLD 4556, Australia. [2]School of Biomedical Sciences, University of Queensland, St. Lucia, QLD 4072, Australia. [3]Department of Biology, Wofford College, Spartanburg, SC 29303, USA.

*Author for correspondence (bob.cieri@gmail.com)

R.L.C., 0000-0001-6905-9148; J.S.M., 0000-0002-8647-4420

Journal of Experimental Biology

1

slow-twitch muscles are primarily involved in slower locomotion or body support. Although the relationship between muscle design and locomotion is complex, this correlation between fCSA and metabolic capacity is generally consistent within individual limb muscles and for different muscles within an organism in several species of lizards (Acevedo and Rivero, 2006; Gleeson and Harrison, 1988; Gleeson et al., 1980; Schiaffino and Reggiani, 2011) and in many, but not all, mammals (Rome and Lindstedt, 1997; but see Bottinelli and Reggiani, 2000).

Adding to this complexity, absolute fCSA differs substantially among individual muscles within an animal (Allen et al., 2014; Cieri et al., 2020; Cuff et al., 2016a; Dick and Clemente, 2016), fibre type distribution varies with muscle size (Eng et al., 2008) and other anatomical and physiological aspects of muscle function vary markedly between species. Thus, to investigate these trade-offs in muscle design, it would be ideal to compare multiple muscles across a large range of body sizes, in animals of similar shape and ecology, and to control for muscle fibre type.

Although few explicit comparisons have been made, the main driver of the difference in overall muscle size among species of different body sizes is presumably muscle fibre number (Rehfeldt et al., 1999). Despite fibre division being restricted to the early stages of development in humans, mosaic hyplerplasia allows fishes to continue recruiting new fibres throughout development (Johnston, 2006; Jorgenson et al., 2020). Data from black sea bass (*Centropristus striata*) suggest that differences in muscle size between relatively small individuals are due mainly to hypertrophy but that hyperplasia becomes more important at greater body sizes (Priester et al., 2011). The relationship between body size and fCSA both within a muscle and within individual fibre types, however, remains unclear. Among other factors, larger animals could theoretically increase muscle force-generating capacity by shifting to a higher proportion of fast-twitch fibres, yet when compared with smaller animals, larger animals generally appear to have more slow-twitch fibres (Schiaffino and Reggiani, 2011). The fact that slower muscle fibres have smaller fCSA than fast fibres (Rome and Lindstedt, 1997) suggests that average fCSA should decrease with body size, but support for this relationship is conflicting.

In mammals, individual muscle fCSA is often reported to either be invariant with body size (Rome and Lindstedt, 1997) or increase with body size generally (Eisenberg, 1983); however, the available morphological evidence suggests (albeit modestly) that fCSA increases with body size. For example, previous studies in mammals report slight positive scaling of individual muscle fCSA ($\propto M_b^{0.05}$) (Hoppeler and Flück, 2002) and diameter ($\propto M_b^{0.02-0.0375}$) (Seow and Ford, 1991). In reptiles, a variety of results for the scaling of muscle fCSA in locomotor muscles have been found (Bonine et al., 2001, 2005; Gleeson, 1983; Gleeson and Harrison, 1986, 1988; Young et al., 1990). In fishes and invertebrates, multiple studies have shown an increase in fibre diameter and reduction in fibre number with body size (Johnston et al., 2003, 2004, 2012).

Unlike results for fCSA, relationships between muscle fibre type and body mass have been more clearly identified in many taxa. In mammals, locomotor muscles are generally composed of fast fibre types (higher glycogen concentration) with higher shortening velocities (v) and maximum shortening velocities (v_{max}) in small animals, with the overall fibre composition becoming slower (lower glycogen concentrations) with increasing body size (reviewed in Schiaffino and Reggiani, 2011; Thomas et al., 1994). Lizards, however, do not show a similar transition from faster to slower muscle fibre phenotypes with increasing body size either within a species (Gleeson and Harrison, 1986) or among species (Bonine

et al., 2001, 2005). In reptiles, three fibre types have been identified: (1) fast-twitch glycolytic (FG) which produce high force, power, v and v_{max}, but fatigue quickly; (2) slow oxidative (SO) fibres that produce lower force and power, v and v_{max}, but fatigue slowly; and (3) fast-twitch oxidative-glycolytic (FOG) fibres which produce intermediate force, v and v_{max}, and power, but have intermediate fatigue resistance (Gleeson and Johnston, 1987; Gleeson et al., 1980; Peter et al., 1972; Rome et al., 1990; Scales et al., 2009). Fast-twitch muscles are activated in varanids for high-speed burst locomotion (Jayne et al., 1990).

The metabolic properties of muscle cells related to fuelling locomotor activity also vary across species and body sizes. Enzymes responsible for glycolytic metabolism (e.g. lactate dehydrogenase) scale positively with body mass within several lizard species, including black spiny-tailed iguanas (*Ctenosaura similis*) (Garland, 1984) and central netted dragons (*Ctenophorus nuchalis*) (Garland and Else, 1987), as well as widely in fishes (Moyes and Genge, 2010). In adult male desert iguanas, however, total muscle enzymatic activity (glycolytic and oxidative combined) decreased with body size (Gleeson and Harrison, 1986). If positive scaling of glycolytic metabolic capacity is present or the percentage of fast-twitch fibres increases, it would enable the maintenance of high sprint speeds with increasing body mass by increasing anaerobic metabolic power for muscle contractions (Somero and Childress, 1980). This may be a compensatory mechanism, in combination with larger muscles, to partially overcome the challenges imposed by geometric scaling in the disparity of muscle force with body mass (Somero and Childress, 1980). Muscle performance characteristics have also been shown to vary with body size in the iliotibialis of lacertid lizards, maximal tetanus strength and muscle power increased, but fatigue resistance decreased with body size (James et al., 2015). Thus, there appears no clear consensus on how we might expect these variables to change with size across different taxonomic groups. Many studies – including several covering substantial body size ranges (Hardy et al., 2010; Jimenez et al., 2008; Kinsey et al., 2007) – report muscle fibre size measurements (e.g. Gleeson and Johnston, 1987; Johnston et al., 2004; Kielhorn et al., 2013; Velten et al., 2013; Gleeson and Harrison, 1986), but a comparative quantitative analysis of these data should provide greater insight into the general patterns regarding how muscle fibre type, muscle glycolytic capacity, or muscle enzyme capacity might be expected to change with size.

Here, we examined the scaling relationships of fCSA and muscle glycogen concentration in 11 hindlimb locomotor muscles from varanid lizards ranging in body mass from 105 g to 40,000 g (fCSA) and 265 g to 4025 g (glycogen concentration). Varanid lizards are an ideal clade for understanding scaling relationships of the musculoskeletal system in response to changes in body mass because they retain similar sprawling posture and locomotor kinematics across an enormous range in body size (Clemente et al., 2011; Dick and Clemente, 2016, 2017; Thompson et al., 1997). Our previous work has shown allometric increases in muscle mass and PCSA with body size in varanid forelimb and hindlimb muscles, however muscle force-generating capacity could also be increased by means of an increased proportion of faster fibre types. We predicted that, given the constraints imposed by the geometric scaling of muscle force: (1) both individual fCSA and fibre number would increase with body size in order to increase the force-generating capacity of locomotor muscles, and (2) muscle glycogen concentration (as an index of muscle fibre type) would increase with body size, reflecting a greater capacity for the higher peak forces with increased body size involved in varanid locomotion

(Cieri et al., 2021). fCSA and glycogen content may also scale more clearly against muscle mass rather than body mass, given that muscle mass has been shown to scale with positive allometry in these animals (Cieri et al., 2020; Dick and Clemente, 2016).

Variation in specimen tissue preservation did not allow us to directly determine muscle fibre type using traditional methods. Instead, we measured muscle glycogen concentration, which represents the amount of fuel within a muscle cell for rapid anaerobic muscle activities that are associated with faster muscle fibre types (reviewed in Schaeffer and Lindstedt, 2013). While not a direct proxy for muscle fibre type, this trait does provide information regarding the glycolytic capacity of a muscle fibre, is generally correlated with fibre type (Burke et al., 1971; Schaart et al., 2004) and should therefore be relatively greater in more glycolytic (fast-twitch) muscle fibres. Finally, our understanding of how muscle architecture traits change with body size generally can best be examined by controlling for phylogenetic independence and comparing traits across multiple clades. We therefore also sought to contextualize our findings in a broader comparative trend by examining how fCSA varies with body size in animals using data available in published literature.

MATERIALS AND METHODS
Animals
Eleven hindlimb muscles (Table 1) were dissected (Fig. 1B) from 15 varanid lizards, ranging in body size from 105 g to 40,000 g (Fig. 1A). Animals (except for *Varanus komodoensis*, which were cadavers from captive animals) were wild caught using a variety of pit trapping, funnel trapping, and hand foraging techniques. Animals that were obviously injured, sick or malnourished were excluded from the study. Lizards were collected under permits WISP11435612 (QLD), SF009075 (WA), 61540 (NT), 08-001092-5 (WA) and WA0001919 (QLD); and ethics SBS/195/12/ARC (QLD), ANA16104 (QLD) and RA/3/100/1188 (WA). The age of animals is not reported as they were largely caught from the wild, but the vast majority of the animals caught were males. No systematic differences in muscle architecture were detected between males and females previously (Dick and Clemente, 2016). The following animals were included for the study of fCSA and glycogen concentration: *Varanus panoptes* (2 individuals:= 997 g; 1060 g), *Varanus tristis* (1 individual: 265 g), *Varanus varius* (3 individuals: 810 g, 834 g, 4025 g).

Additional data were collected from these animals: *Varanus gouldii* (3 individuals: 429 g, 439 g, 459 g), *V. komodoensis* (2 individuals: 30,000 g, 40,000 g), *V. panoptes* (2 individuals: 1060 g, 2077 g), *Varanus scalaris* (1 individual: 158 g), *V. tristis*

(1 individual: 265 g), *V. varius* (3 individuals: 810 g, 834 g, 4025 g), which may have been frozen at least once before analysis. Whole muscles were dissected and weighed. Fresh animals were fasted for 24 h prior to being euthanized.

Anatomical methods
During dissections, the whole muscle was excised and relevant muscle parameters were measured (Dick and Clemente, 2016). Next, the mid-belly of the muscle was determined to be half the distance between the origin and the insertion. The muscle was cut perpendicular to the fibre orientation at two points approximately 0.5 cm apart. This section was then fixed in 10% formalin and then dehydrated in ethanol. Each sample was mounted in a tissue cassette, oriented perpendicular to the long axis of the muscle and embedded in wax. Oblique sections of muscle fibres were identified where diameter in one axis was more than twice the diameter in the perpendicular axis and excluded from the analysis. Wax-mounted muscles were thin-sliced (1 μm) and mounted onto glass slides. Slides were rehydrated and stained for glycogen using the stains and protocol in a commercial periodic acid-Schiff kit (Sigma-Aldrich 395B-1KT). Briefly, the staining protocol was as follows: slides were incubated at 60°C for 30 min in an oven to melt the wax covering, and then deparaffinized and hydrated. Hydration consisted of the following steps with the slides vertically mounted in plastic slide staining racks and solutes in successive wells of a 12-well slide staining dish: submersion in xylene (twice for 5 min), submersion in 100% ethanol (twice for 5 min), and submersion in 80% ethanol (twice for 5 min). Still in the vertical slide staining racks and using the staining dish wells, slides were then immersed in periodic acid solution (1 g dl^{-1} H$_2$O) for 5 min, rinsed in several changes of deionized water, immersed in Schiff's reagent for 15 min, and washed in running tap water for 5 min. Slides were then removed from the vertical staining racks, and hematoxylin solution (gill no. 3) was applied for 90 s with a plastic transfer pipette. Slides were then rinsed in running tap water, dehydrated back to xylene using a reverse of the hydration protocol in vertical staining racks (80% ethanol twice for 5 min, 100% ethanol twice for 5 min, and xylene twice for 5 min), and a slide cover was immediately applied with slide adhesive.

Photographs of slides were taken at 40× or 100× magnification using a Nikon Eclipse E200 light microscope and a Basler acA1920-150uc USB area scan camera (Basler AG, Arhrensburg, Germany). Muscle fibre areas were calculated in ImageJ (v.1.53a, National Institutes of Health) using the hand-traced polygon selection tool after the field of view was calibrated to a 1000 μm length scale at each magnification using a calibration slide.

Table 1. Muscles investigated in this study

Muscle	Abbreviation	Primary function	fCSA		Glycogen concentration	
			N slides	n individuals	N slides	n individuals
Caudofemoralis longus	cFem	Femur retraction	12	10	5	5
Iliofemoralis	ilFem	Femur abduction	10	10	5	5
Flexor tibialis internus (deep head)	FTIdeep	Knee flexion	10	10	5	5
Flexor tibialis internus (superficial head)	FTIsup	Knee flexion	11	10	6	6
Iliofibularis	ilFib	Knee flexion	28	15	5	5
Pubotibialis	pTib	Knee flexion	11	10	5	4
Iliotibialis	ilTib	Knee extension	14	13	5	5
Femorotibialis	femTib	Knee extension	10	10	5	5
Gastrocnemius	gast	Ankle plantar flexion	18	15	6	5
Peroneus longus	pLong	Ankle plantar flexion	13	11	8	6
Tibialis anterior	tibAnt	Ankle dorsiflexion	29	15	11	6

Muscles are described in detail in Dick and Clemente (2016) and shown in Fig. 1B. fCSA, fibre cross-sectional area.
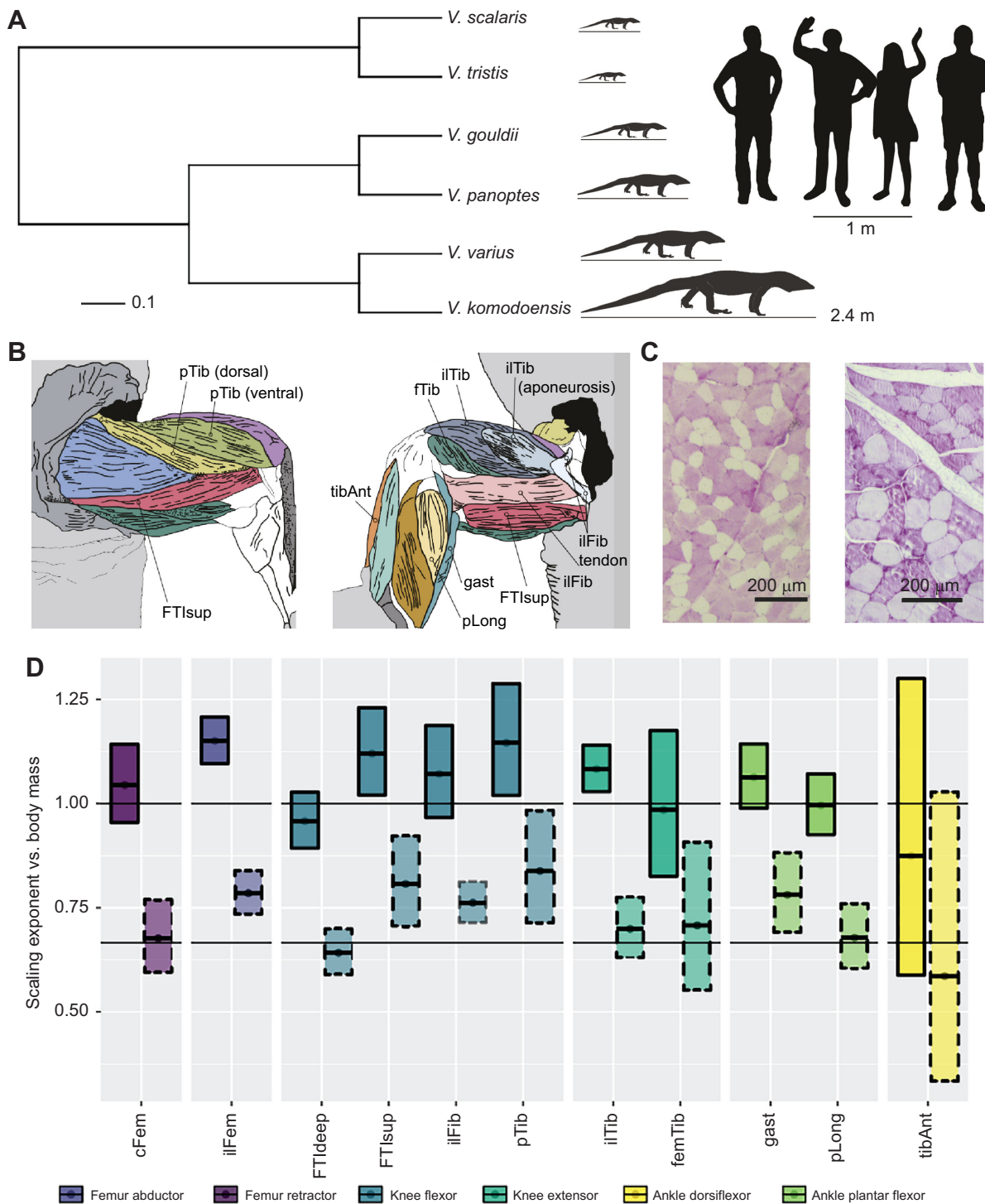
Fig. 1. Cladogram, anatomy and scaling of parameters for studied varanid lizard species and muscles. (A) Cladogram of included *Varanus* spp. with images of the authors to scale. (B) Anatomical locations of hindlimb muscles included in the study shown from superficial dorsal (left) and deep ventral (right) views. (C) Representative micrographs of stained femTib (left) and tibAnt (right) sections from a 1060 g *V. panoptes*. (D) Scaling exponents for muscle mass (solid) and physiological cross-sectional area (PCSA) (dotted) versus body mass for muscles examined in this study. Boxes represent the means and 95% confidence intervals. A, B and E adapted from Dick and Clemente (2016). All muscle abbreviations and sample sizes as listed in Table 1.

The areas of 10 fibres were calculated in four different, randomly selected regions on each muscle slide from 1–4 slides per muscle per individual. Fibre areas were calculated instead of fibre diameters because they are more directly related to changes in muscle force output, which relates to whole muscle physiological cross-sectional area (the cross-sectional area of muscles perpendicular to muscle

fibre). In only slides where staining led to clear differentiation, fibre counts were performed using the multipoint tool in ImageJ. In four different regions of each muscle, the dark, medium and light fibres were counted, corresponding to high, medium and low glycogen concentrations, respectively. Other muscle parameters, including PCSA, muscle mass and fascicle length were measured previously

(Cieri et al., 2020; Dick and Clemente, 2016). All fCSA values were multiplied by a conversion factor of 1.63212 to account for the reduction in fibre cross-sectional area that occurs as a result of 1 month of ethanol storage according to published decay equations (Leonard et al., 2021a,b). Storage in ethanol for 1 month after fixation in formalin causes a decrease in muscle mass of 41% compared with fresh tissue (Leonard et al., 2021a) and reductions in fCSA relate to reductions in muscle mass over longer periods by a reduced major axis regression [relative fCSA=(relative muscle mass×10,113.5)+5.9272; R^2=0.9648] (Leonard et al., 2021b) such that fCSA can be expected to decrease by 61.27%. To control for differences in specimen preparation, fCSA was calculated among all samples, and also among a subset of the data where specimens were never frozen prior to analysis. Incorrect freezing of tissue can lead to the formation of larger ice crystals which dehydrate muscle fibres, leading to underestimates of fibre area (Leonard et al., 2021a). Thus, scaling exponents calculated from all samples may provide an underestimate, but cover a much wider range of body sizes, while the fresh samples may yield more accurate exponents but cover a narrower range of body sizes.

For the comparative analysis, fibre areas and body masses were taken from the literature for mammals (Hoppeler and Flück, 2002; Kielhorn et al., 2013; Kroeger et al., 2020; Marx et al., 2006; Seow and Ford, 1991; Velten et al., 2013), birds (Brown et al., 2019), phrynosomatid lizards (Bonine et al., 2005), as well as fish and invertebrates (Jimenez et al., 2013). Fibre diameters were converted into areas assuming a circular shape. For birds, data from the domestic chicken (*Gallus domesticus*) were excluded because the pectoralis muscle architecture of this species has likely been under intense artificial selection. In cases where fast and slow muscle fibre areas were provided for the same individual, these were averaged. In cases where the original articles provided details about muscle preservation, appropriate correction factors were calculated as above using regressions from Leonard et al. (2021a,b).

Statistical methods
Statistical analyses were conducted using R 3.6.3 (https://www.r-project.org/). The relationships between anatomical parameters (body mass, muscle mass, muscle physiological cross-sectional area, fascicle length) and histological parameters (fCSA, proportion of low-glycogen fibres) were assessed using mixed effects models (LMMs) using the lmer.R function from the lme4 package (https://CRAN.R-project.org/package=lme4), including animal (individual) nested within species as a random factor (Bates et al., 2015). To investigate the overall scaling relationships of all muscle fibres together, muscle was also included as a random factor. The scaling of muscle fibre number was calculated by dividing the scaling of total muscle cross-sectional area by the scaling of fCSA. As a conservative measure, the relative proportion of low-glycogen content fibres only was analysed and was calculated as the ratio of light-stained category fibres over total counted stained fibres. All continuous variables were log-transformed to promote normality and homoscedasticity in data distribution. Ratio values are not log-transformed and scaling exponents for these variables are from semi-log regressions. Individual fixed effect regression slopes (Table 2) were extracted using sim_slopes.R and plotted using interact_plot.R from the interactions package (https://CRAN.R-project.org/package=interactions). Intercepts (Table 2) were calculated directly from the mixed effects model outputs. Effect sizes for LMMs are presented as η^2 from the t_to_eta2.R function from the effectsize package (Ben-Shachar et al., 2020). Other relationships were tested using Kruskal–Wallis tests, and *post hoc* comparisons were made with Dunn's tests with Bonferroni corrections using the dunn.test package (https://CRAN.R-project.org/package=dunn.test). For the comparative analysis, mixed effects models were used to investigate the relationship between body size and fCSA for each taxonomic group, holding species as a random effect.

Phylogenetically-corrected slopes for fCSA data were calculated using the gls.R function from the nlme package in R (https://CRAN.R-project.org/package=nlme), under the assumption of correlation= corBrownian(1,tree). Brownian motion was chosen over early burst, Ornstein–Uhlenbeck or Lambda models as the evolutionary model because it was best supported based on AIC. A phylogenetic tree containing all species (Fig. S1) was created from the Timetree database (Kumar et al., 2017). Where body masses are not reported for mammals, these were estimated from Pacifici et al. (2013). *Post hoc* comparisons between groups in the gls models were calculated using the posthoc.R function from the package postHoc (https://CRAN.R-project.org/package=postHoc).

Table 2. log–log scaling coefficients for physiological cross-sectional area (PCSA) and fibre cross-sectional area (fCSA) versus log body mass among varanid muscles

| Muscle | PCSA (cm^2) | | | | fCSA (μm^2) | | | |
| | Slope | | | Intercept | Slope | | | Intercept |
	Lower	Mean	Upper		Lower	Mean	Upper	
All	0.635	0.707	0.780	−2.46	0.156	0.197	0.237	3.15
cFem	0.583	0.647	0.710	−1.34	0.048	0.145	0.241	3.37
ilFem	0.719	0.781	0.845	−2.89 *	0.016	0.111	0.207	3.11
FTIsup	0.655	0.728	0.800	−2.54 *	0.126	0.239	0.352	3.09
FTIdeep	0.536	0.599	0.662	−2.48 *	0.014	0.108	0.203	3.27
ilFib	0.736	0.796	0.857	−2.81 *	0.092	0.181	0.270	3.19
pTib	0.710	0.780	0.849	−2.82 *	0.063	0.164	0.266	3.27
ilTib	0.622	0.685	0.749	−2.49 *	0.048	0.145	0.241	3.27
femTib	0.698	0.764	0.831	−2.55 *	0.169	0.270	0.372	3.09*
gast	0.721	0.788	0.855	−2.31 *	0.222	0.324	0.427	2.80*
pLong	0.649	0.718	0.788	−2.49 *	0.148	0.249	0.350	2.98*
tibAnt	0.520	0.580	0.639	−2.31 *	0.155	0.243	0.331	2.86*

Values represent independent fixed-effects coefficients calculated from linear mixed effects models and 95% confidence intervals using all reported data. Slopes and intercepts for all muscles were calculated using a mixed effects model holding animal and muscle as random effect. All slopes are significant with $P<0.05$.
*Intercept is significantly different ($P<0.05$) from the intercept for cFem.

RESULTS

Across all individuals, the smallest fibres were found in tibialis anterior (tibAnt; 3945±1939 µm^2), and the largest fibres were found in femorotibialis (femTib; 10,169±5262 µm^2). Raw and body size-normalized values are shown in Table S1. fCSA scaled positively with body mass taking all muscles together among all samples ($\propto M_b^{0.197}$ LMM; d.f.=128.6, η^2=0.42, P<0.0001; body size: 104.5–40,000 g) and among a smaller range of body sizes representing fresh samples only ($\propto M_b^{0.278}$ LMM; d.f.=53.19, η^2=0.34, P<0.0001; body size: 845–4025 g). Considering each muscle separately, fCSA scaled positively with body mass in all muscles (Fig. 2, Table 3). Among fresh samples, fCSA scaled positively with body mass in all muscles except for the caudofemoralis longus (cFem) and iliotibialis (ilTib). Among all samples, whole muscle cross-sectional area (PCSA) scaled $\propto M_b^{0.708}$ (LMM; d.f.=13.19, η^2=0.97, P=0.001) so the number of muscle fibres therefore scaled $\propto M_b^{0.511}$ assuming that all increases in PCSA were due to fCSA or fibre number. Among the smaller range of body sizes representing fresh samples only, whole muscle cross-sectional area scaled $\propto M_b^{0.673}$ (LMM; d.f.=10.79, η^2=0.97, P=0.001) so the number of muscle fibres therefore scaled $\propto M_b^{0.395}$ assuming that all increases in PCSA were due to changes in fCSA or fibre number. PCSA increased with fCSA among all samples (log–log slope: 0.377, LMM; d.f.=504.35, η^2=0.03, P<0.0001; Fig. 3) and among a smaller range of body sizes representing fresh

samples only (log–log slope: 0.454, LMM; d.f.=214.08, η^2=0.05, P<0.005).

When muscle data from multiple taxonomic groups were aggregated and regressed in a phylogenetic framework, fCSA was found to scale $\propto M_b^{0.182}$ (GLS; P<0.0001). We further compared the scaling of fCSA between groups (GLS; P<0.001), finding that the scaling exponent was different between groups (Fig. 4, Table 3). fCSA scaled much more steeply with body mass in invertebrates ($\propto M_b^{0.575}$) than in other groups, more steeply in fish ($\propto M_b^{0.347}$) and non-varanid reptiles ($\propto M_b^{0.308}$) than in varanids ($\propto M_b^{0.267}$). fCSA scales still more steeply with body mass in varanids, than in birds (pectoralis muscle only) ($\propto M_b^{0.134}$) and mammals ($\propto M_b^{0.122}$). Significant differences in scaling exponents were detected using *post hoc* comparisons between invertebrates and mammals (P=0.014), and birds and invertebrates (P=0.022).

There was no significant relationship between the proportion of low-glycogen fibres with either body mass or muscle mass when all muscles were considered together in linear mixed effects models where animal and muscle were held as random effects. When muscle was included as a fixed effect, the proportion of low-glycogen fibres decreased significantly with body mass in the iliofibularis (ilFib; semi-log slope: −49.25; LMM; d.f.=175.83, η^2=0.09, P=0.001) and femTib (semi-log slope: −36.40; LMM; d.f.=179.94, η^2=0.06, P=0.011).
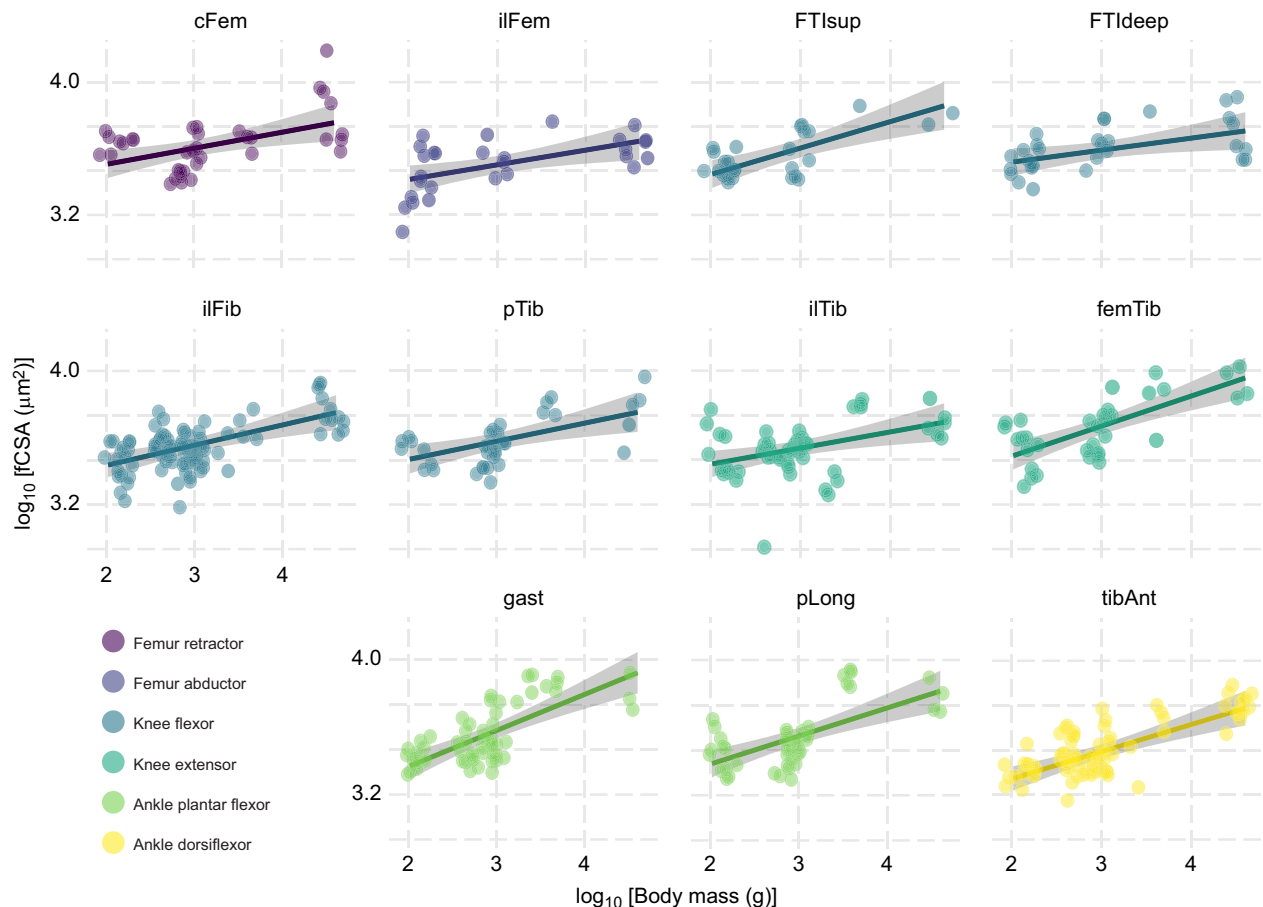
Fig. 2. Scaling of single muscle fibre cross-sectional area (fCSA) versus body mass. Regression lines (LMM; P<0.05 for all plots) and confidence intervals for each muscle from mixed effects models. Slopes and intercepts are shown in Table 3, and sample sizes given in Table 1. Colours indicate primary muscle functions. All muscle abbreviations as listed in Table 1.

Table 3. Scaling coefficients for log$_{10}$ fibre cross-sectional area (µm^2) versus log$_{10}$ body mass (g) among broad taxonomic groups

		Species mean LMM regression		Phylogenetically corrected GLS regression	
		Slope	Intercept	Slope	Intercept
All species	Upper	0.115	3.720	0.232	4.95
	Mean	**0.052**	**3.607**	**0.182**	**4.267**
	Lower	−0.010	3.495	0.133	3.584
Invertebrates	Upper	0.834	6.107	0.282	6.629
	Mean	**0.619**	**5.672**	**0.575**	**5.578**
	Lower	0.408	5.521	0.868	4.526
Fishes	Upper	0.567	4.524	0.710	5.568
	Mean	**0.459**	**4.347**	**0.347**	**4.145**
	Lower	0.333	4.162	−0.017	2.722
Varanid lizards	Upper	0.723	3.891	0.578	5.199
	Mean	**0.346**	**3.676**	**0.267**	**3.671**
	Lower	0.191	3.487	−0.044	2.143
Other lizards	Upper	0.459	4.390	0.638	5.516
	Mean	**0.297**	**4.066**	**0.308**	**4.018**
	Lower	0.135	3.742	−0.021	2.520
Birds	Upper	0.140	3.188	0.466	4.652
	Mean	**0.087**	**3.112**	**0.134**	**3.135**
	Lower	0.034	3.037	−0.199	1.619
Mammals	Upper	0.092	3.492	0.422	4.873
	Mean	**0.050**	**3.397**	**0.122**	**3.362**
	Lower	0.008	3.302	−0.178	1.851

Raw species mean coefficients were calculated using linear mixed effects models where species was held as a random effect. Phylogenetically corrected coefficients were calculated from species means using a phylogenetically corrected generalized least squares regression. Significance for all slopes and means: $P<0.01$.

fCSA within each glycogen content category (low, medium, high) were also found to increase with body size: low-glycogen category fibres ($\propto M_{b}^{0.330}$ LMM; d.f.=54.06, η^2=0.09, $P<0.05$), medium-glycogen category fibres ($\propto M_{b}^{0.317}$ LMM; d.f.=55.31, η^2=0.09, $P<0.05$) and high-glycogen category fibres ($\propto M_{b}^{0.269}$ LMM; d.f.=55.05, η^2=0.07, $P<0.05$). When the fCSA for each glycogen concentration category was multiplied by the proportion of that category to form a weighted average, all fibres together scaled ($\propto M_{b}^{0.337}$ LMM; d.f.=187.00, η^2=0.11, $P<0.001$).

Muscle fCSA was significantly smaller in low-glycogen (1.10±0.11 µm^2) than either medium (1.15±0.10 µm^2) or high-glycogen (1.14±0.10 µm^2) fibres (χ^2=25.24, d.f.=2, $P<0.001$). Pairwise comparisons indicated significant differences in fCSA between all glycogen concentration fibre groups.

DISCUSSION

Here, we report the scaling of muscle fibre cross-sectional area (fCSA) in 11 hindlimb locomotor muscles of varanid lizards ranging in body mass from 105 g to 40,000 g and muscle glycogen concentration in 11 muscles of varanid lizards ranging in body mass from 265 g to 4025 g. The first main finding of this study is that muscle fCSA increased with body mass ($\propto M_{b}^{0.278-0.197}$), corresponding to a scaling of fibre diameter $\propto M_{b}^{0.140-0.099}$. This finding supports our main hypothesis that increases in fCSA (analogous to hypertrophy) would contribute along with increases in fibre number (analogous to hyperplasia) to allometric increases in muscle PCSA with body size. The true scaling exponent is likely above the lower presented value because it is calculated from a dataset that includes once-frozen animals of higher body size, and the muscles from these animals may have shrunk because of dehydration before analysis (Leonard et al., 2021a). The true exponent may be

closer to the higher presented value because this exponent was calculated using animals that were never frozen, but is based on data from animals covering a substantially smaller range of body sizes. Increases in fCSA made less of a contribution than increases in fibre number (analogous to hyperplasia). However, this increase is not due solely to changes in fibre type, as we also show that fCSA increases independently in fibres with high, low and medium levels of glycogen. These results are consistent with previous studies that also display increased fCSA in the iliofibularis muscle with body mass in lizards (Bonine et al., 2001, 2005; Gleeson and Harrison, 1986). On the other hand, Gleeson and Harrison (1988), found that fCSA increased with body size in *Dipsosaurus* in the fast glycolytic fibres of the gastrocnemius only, with no relationship in the iliofibularis or caudofemoralis. In our data, fCSA increased with body size in the iliofibularis and caudofemoralis, but scaling exponents for these muscles were among the lowest of all muscles.

Increases in fCSA partially compensate for the disproportionally higher force requirements of locomotion and body support at larger body sizes. As geometrically similar sprawling animals increase in size, force production should scale $\propto M_{b}^{0.67}$ as it depends on muscle cross-sectional area, while locomotor forces should scale $\propto M_{b}^{1}$ because they depend on animal mass. Thus, larger animals must become relatively stronger or change shape to locomote similarly to smaller animals. In varanid lizards, which do not change substantially in overall shape or posture (Clemente et al., 2011), peak ground reaction forces scale $\propto M_{b}^{0.89-0.99}$ (Cieri et al., 2021) and while PCSA and mass of the forelimb and hindlimb muscles scales with positive allometry, this is not sufficient to fully explain the scaling of ground reaction forces. An increased fCSA means that muscle fibres should generate more total force because of a greater number of sarcomeres in parallel (Bruce et al., 1997; Krivickas et al., 2011). Force per unit cross-sectional area in the iliofibularis of *Sceloporus torquatus* is greater in males, which are larger than females and have fibres with higher fCSA, even though the relative proportion of fibre types is not different between sexes (Quintana et al., 2014).

The implications of increased fCSA for sprint speed, however, are much less straightforward. Even though larger fCSA is associated with greater force production (Krivickas et al., 2011; Quintana et al., 2014), fCSA in the iliofibularis has been shown to be negatively correlated with sprint speed, despite being the best predictor of it, in adult male desert iguanas (Gleeson and Harrison, 1988). This could be due to a trade-off in muscle design, whereby larger fibres produce more force, but at the cost of decreased oxidative capacity (owing to limitations in the speed of oxygen diffusion) and, thus, decreased efficiency and endurance (Kinsey et al., 2007, 2011). If short-term fatigue due to muscle fibre diffusion limitations is present, the larger fCSA may partially explain the lower sprint speeds in desert iguanas (Gleeson and Harrison, 1988) and with body size in varanids (Clemente et al., 2009b) by imposing an upper limit on sustained locomotor activity through an increase in the fatigability of muscle fibres. A considerable body of work has shown, however, that most animal muscle fibres grow and are organized to avoid theoretical diffusion limitations, but are instead limited by reaction rates (Kinsey et al., 2007, 2011). If this is the case, fCSA may be responding more to changes in body mass in varanids, and sprint speed may instead be limited by safety factors imposed by the musculoskeletal system (Cieri et al., 2021; Clemente et al., 2011; Dick and Clemente, 2017).

Our second main finding, that fCSA increases generally with body size in different groups, but much more steeply in fishes and invertebrates, more steeply in non-varanid lizards and somewhat
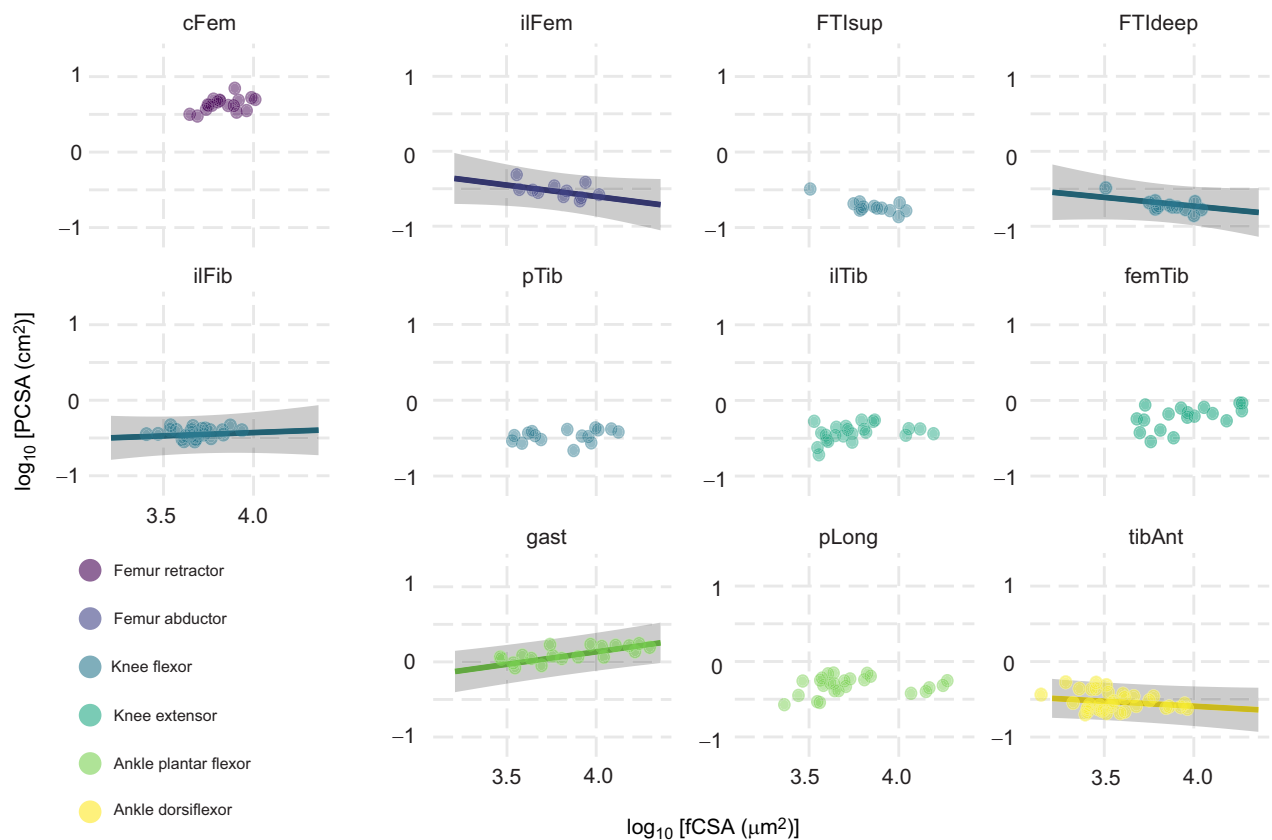
Fig. 3. Scaling of whole-muscle physiological cross-sectional area (PCSA) versus single muscle fibre cross-sectional area (fCSA). Regression lines and confidence intervals for each muscle from mixed effects models with equations listed in Table 2 and sample sizes listed in Table 1. Colours indicate primary muscle functions. Scaling for all muscles combined (log–log slope: 0.377; LMM; $P<0.0001$). All muscle abbreviations as listed in Table 1.

more steeply in varanids (Fig. 4), provides broad comparative insights into the locomotor consequences of increased fCSA. The optimal fibre size hypothesis suggests that larger fibres may be metabolically optimal because the lower surface area to volume ratio in larger fibres reduces the metabolic cost of maintaining the resting membrane potential (Jimenez et al., 2011, 2013; Johnston et al., 2003, 2004, 2006). In smaller muscle fibres, the cost per muscle contraction is lower but the considerable costs (Milligan and McBride, 1985; Zurlo et al., 1990) associated with maintaining the membrane potential are greater (Jimenez et al., 2013). This may be advantageous in endothermic mammals and birds, which maintain a higher basal metabolic rate and move more regularly (Bennett and Ruben, 1979; Farmer, 2003, 2020). Ectotherms, such as reptiles and invertebrates, however, which have lower basal metabolic rates and move less frequently, may benefit from larger muscle fibres that cost more to contract but have lower costs of membrane potential maintenance (Jimenez et al., 2013). Under this paradigm, the scaling exponent of varanids, which is higher than in birds and mammals but lower than in other reptiles may be explained by the elevated maximal metabolic rates of varanids compared with other reptiles (Clemente et al., 2009a; Thompson et al., 1997). Similarly, the steeper scaling of fCSA with body size in fishes and invertebrates (most species with published fCSA values are marine) may also reflect habitat differences, as the muscle activation necessary to support the body against gravity in terrestrial animals may select for smaller fibres with relatively lower contraction costs at the expense of higher maintenance costs.

The third main finding is that the proportion of fibres in the low-glycogen category decreases with body size in some varanid

hindlimb muscles, lending conditional support to our hypothesis. Although glycogen staining is only a proxy of fibre type, these data suggest that these muscles may be composed of relatively more fast-twitch muscle fibres in larger varanids. Muscles composed of proportionally more fast-twitch fibres should produce more force, helping to close the gap between theoretical predictions of muscle force ($\propto M_b^{0.67}$) and observed peak ground reaction forces ($\propto M_b^{0.89-0.99}$). In other muscles in our study, however, glycogen concentration does not change with body size, suggesting that the value of disproportionate increases in force at higher body sizes differs between muscles. It may also suggest that slow-twitch fibres (likely the postural muscles) become more valuable in certain muscles at larger body sizes, perhaps because they are more resistant to fatigue and cost less energy to contract. Future work either directly measuring or simulating the roles of locomotor muscles across a range of body size may make more sense of these patterns.

Finally, a consideration of how animals grow may help to explain the pattern in our data. In mammals, muscle cell division seems to be restricted to the early stages of developmental growth (reviewed in Jorgenson et al., 2020), while cell division also occurs later in development in fishes, termed mosaic hyperplasia (Johnston, 2006, 2003). Thus, although exogenous factors substantially influence muscle growth (e.g. Xu et al., 2021), muscle design can nonetheless be understood as a compromise between the biomechanical needs of the adult and juvenile. Without substantial mosaic hyperplasia, increases in muscle force output to maintain functional similarity during growth must be accomplished in one of two ways. One option, a shift in the proportions of muscle fibre types in larger species towards
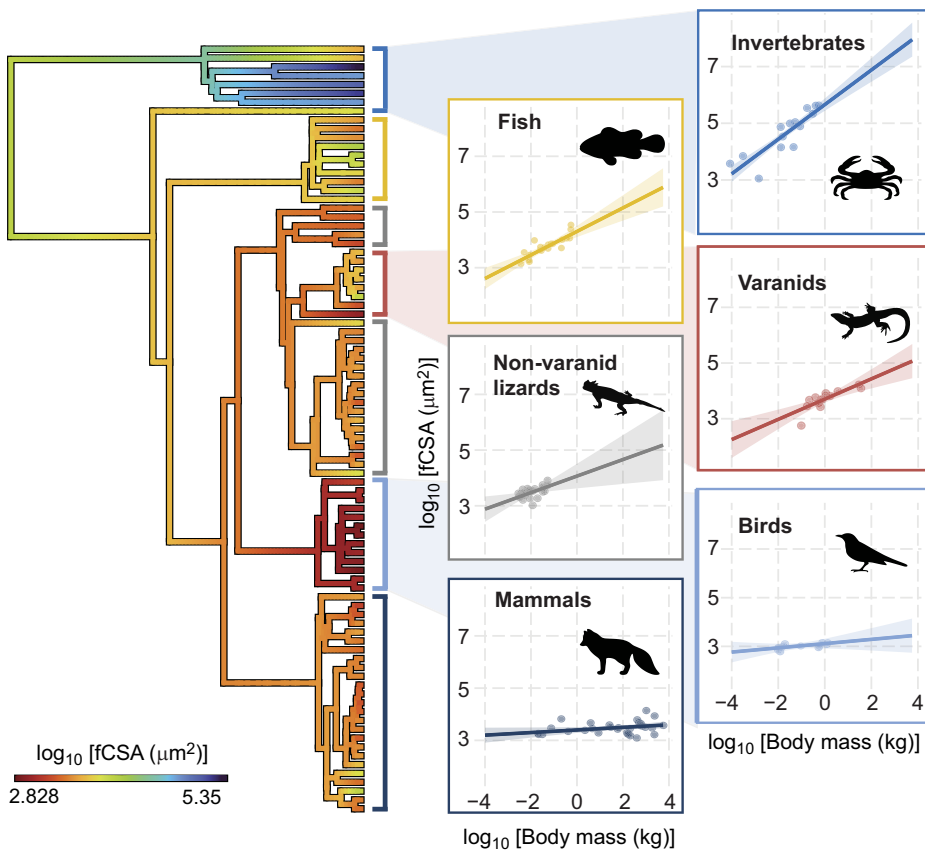
Fig. 4. Scaling of average muscle fibre cross-sectional area (fCSA) from different taxonomic groups. Plots were generated from a linear mixed effects model (LMM, $P<0.05$ for all plots) where animal (individual) nested within species was held as a random effect. Invertebrates ($n=14$), fishes ($n=19$), non-varanid lizards ($n=24$, tibAnt), varanids ($n=15$, species averages of data in this study), birds ($n=13$, pectoralis), mammals ($n=32$, including a combination of whole-body averages, soleus and extensor digitorum longus). The cladogram was generated using the contMap.R function from phytools package in R and represents the estimated ancestral reconstruction of fCSA, with smaller fibres represented in red colours, and larger fibres in blue.

glycolytic (fast-twitch) fibres would increase total muscle force output. Our glycogen content scaling data suggest that varanids use this pattern in some (but not all) muscles, so perhaps the need for mainly aerobic muscle fibres in the juveniles (which have higher relative maximal metabolic rates than adults) (Clemente et al., 2008; Thompson, 1996) of larger varanid species outweighs the advantage that the more forceful and powerful glycolytic fibres would provide the adults in other muscles. The second option for increasing total muscle force output is through proliferation of myofibrils within muscle cells, leading to hypertrophy and increased fCSA, which also occurs in varanids. In black sea bass, muscle fibre diameter increased substantially from 36 µm to 280 µm (corresponding roughly to fCSA of 1017–61,544 µm²) in individuals between 0.45 g and 2000 g, but increases in muscle size from individuals ranging from 2000 to 4840 g in body mass were accomplished through increased recruitment of smaller fibres (Priester et al., 2011). Fibres also increased in area along a similar range of body sizes in varanids, but the highest raw fCSAs in varanids were not as large as in sea bass, and there was no obvious body size in varanids where further increases in fCSA were solely due to changes in fibre number as in sea bass. This comparison suggests that larger fibres provide a greater advantage with size compared with small fibres in fish versus varanids. It may also indicate that the biomechanical advantages of larger fibres are similar in both groups but become more important at smaller body sizes in fish. A future ontogenetic analysis of muscle design and growth patterns could help to disentangle the effects of individual growth and interspecific size differences.

Concluding remarks

This study provides a more nuanced view of how the musculoskeletal system of varanid lizards responds to the biomechanical challenges of increasing body size. Previous work on scaling in varanids has shown that many hindlimb and forelimb muscles scale with positive allometry for PCSA, fascicle length, and muscle mass to deal with the size-related increases in stress imposed by geometric scaling (Cieri et al., 2020; Dick and Clemente, 2016). Taken together with this previous work, our results suggest that the increase in muscle mass is at least partially accomplished through an increase in muscle fCSA, rather than through an increase in muscle fibre number alone. Our results also suggest that relative increases in fast-twitch muscle fibres, or at least high-glycogen content fibres, may be another mechanism that larger animals use to deal with the outsized force requirements at larger body sizes. These data also suggest that, while fCSA generally increases with body size, the extent of this scaling has taken a different form in different clades, and may relate to broad differences in locomotor function, habitat and activity metabolism between endotherms and ectotherms.

Author contributions
Conceptualization: R.C., T.J.D., C.J.C.; Methodology: R.C., C.J.C.; Formal analysis: R.C.; Investigation: R.C., C.J.C.; Data curation: R.C., C.J.C.; Writing - original draft: R.C.; Writing - review & editing: R.C., T.J.D., J.S.M., C.J.C.; Visualization: R.C.; Supervision: C.J.C.; Project administration: C.J.C.; Funding acquisition: T.J.D., C.J.C.

References

Acevedo, L. M. and Rivero, J. L. L. (2006). New insights into skeletal muscle fibre types in the dog with particular focus towards hybrid myosin phenotypes. *Cell Tissue Res.* **323**, 283-303. doi:10.1007/s00441-005-0057-4

Allen, V. R., Molnar, J., Parker, W., Pollard, A., Nolan, G. and Hutchinson, J. R. (2014). Comparative architectural properties of limb muscles in Crocodylidae and Alligatoridae and their relevance to divergent use of asymmetrical gaits in extant Crocodylia. *J. Anat.* **225**, 569-582. doi:10.1111/joa.12245

Bates, D., Mächler, M., Bolker, B. M. and Walker, S. C. (2015). Fitting linear mixed-effects models using lme4. *J. Stat. Softw.* **67**, 1-48. doi:10.18637/jss.v067.i01

Ben-Shachar, M., Lüdecke, D. and Makowski, D. (2020). effectsize: estimation of effect size indices and standardized parameters. *J. Open Source Softw.* **5**, 2815. doi:10.21105/joss.02815

Bennett, A. F. and Ruben, J. A. (1979). Endothermy and activity in vertebrates. *Science* **206**, 649-654. doi:10.1126/science.493968

Biewener, A. A. (1989). Scaling body support in mammals: limb posture and muscle mechanics. *Science* **245**, 45-48. doi:10.1126/science.2740914

Biewener, A. A. (2005). Biomechanical consequences of scaling. *J. Exp. Biol.* **208**, 1665-1676. doi:10.1242/jeb.01520

Biewener, A. A. and Patek, S. N. (2018). Movement on land. In *Animal Locomotion*, pp. 61-89. Oxford University Press

Bonine, K. E., Gleeson, T. T. and Garland, T. (2001). Comparative analysis of fiber-type composition in the iliofibularis muscle of phrynosomatid lizards (Squamata). *J. Morphol.* **250**, 265-280. doi:10.1002/jmor.1069

Bonine, K. E., Gleeson, T. T. and Garland, T. (2005). Muscle fiber-type variation in lizards (Squamata) and phylogenetic reconstruction of hypothesized ancestral states. *J. Exp. Biol.* **208**, 4529-4547. doi:10.1242/jeb.01903

Bottinelli, R. and Reggiani, C. (2000). Human skeletal muscle fibres: molecular and functional diversity. *Prog. Biophys. Mol. Biol.* **73**, 195-262. doi:10.1016/S0079-6107(00)00006-7

Bottinelli, R., Canepari, M., Reggiani, C. and Stienen, G. J. (1994). Myofibrillar ATPase activity during isometric contraction and isomyosin composition in rat single skinned muscle fibres. *J. Physiol.* **481**, 663-675. doi:10.1113/jphysiol.1994.sp020472

Brown, K., Jimenez, A. G., Whelan, S., Lalla, K., Hatch, S. A. and Elliott, K. H. (2019). Muscle fiber structure in an aging long-lived seabird, the black-legged kittiwake (*Rissa tridactyla*). *J. Morphol.* **280**, 1061-1070. doi:10.1002/jmor.21001

Bruce, S. A., Phillips, S. K. and Woledge, R. C. (1997). Interpreting the relation between force and cross-sectional area in human muscle. *Med. Sci. Sports Exerc.* **29**, 677-683. doi:10.1097/00005768-199705000-00014

Burke, R. E., Levine, D. N., Zajac, F. E., Tsairis, P. and Engel, W. K. (1971). Mammalian motor units: physiological-histochemical correlation in three types in cat gastrocnemius. *Science* **174**, 212-709. doi:10.1126/science.174.4010.709

Cieri, R. L., Dick, T. J. M. and Clemente, C. J. (2020). Monitoring muscle over three orders of magnitude: Widespread positive allometry among locomotor and body support musculature in the pectoral girdle of varanid lizards (Varanidae). *J. Anat.* **237**, 1114-1135. doi:10.1111/joa.13273

Cieri, R. L., Dick, T. J. M., Irwin, R., Rumsey, D. and Clemente, C. J. (2021). The scaling of ground reaction forces and duty factor in monitor lizards: implications for locomotion in sprawling tetrapods. *Biol. Lett.* **17**, 20200612. doi:10.1098/rsbl.2020.0612

Clemente, C. J., Withers, P. C. and Thompsonl, G. G. (2008). Higher than predicted endurance for juvenile goannas (Varanidae; Varanus). *J. R. Soc. West. Aust.* **91**, 265-267.

Clemente, C. J., Withers, P. C. and Thompson, G. G. (2009a). Metabolic rate and endurance capacity in Australian varanid lizards (Squamata: Varanidae: Varanus). *Biol. J. Linn. Soc.* **97**, 664-676. doi:10.1111/j.1095-8312.2009.01207.x

Clemente, C. J., Thompson, G. G. and Withers, P. C. (2009b). Evolutionary relationships of sprint speed in Australian varanid lizards. *J. Zool.* **278**, 270-280. doi:10.1111/j.1469-7998.2009.00559.x

Clemente, C. J., Withers, P. C., Thompson, G. G. and Lloyd, D. (2011). Evolution of limb bone loading and body size in varanid lizards. *J. Exp. Biol.* **214**, 3013-3020. doi:10.1242/jeb.059345

Clemente, C. J., Withers, P. C., Thompson, G. G. and Lloyd, D. (2013). Lizard tricks: overcoming conflicting requirements of speed versus climbing ability by altering biomechanics of the lizard stride. *J. Exp. Biol.* **216**, 3854-3862. doi:10.1242/jeb.089060

Cuff, A. R., Sparkes, E. L., Randau, M., Pierce, S. E., Kitchener, A. C., Goswami, A. and Hutchinson, J. R. (2016a). The scaling of postcranial muscles in cats (Felidae) I: forelimb, cervical, and thoracic muscles. *J. Anat.* **229**, 128-141. doi:10.1111/joa.12477

Cuff, A. R., Sparkes, E. L., Randau, M., Pierce, S. E., Kitchener, A. C., Goswami, A. and Hutchinson, J. R. (2016b). The scaling of postcranial muscles in cats (Felidae) II: hindlimb and lumbosacral muscles. *J. Anat.* **229**, 142-152. doi:10.1111/joa.12474

Dick, T. J. M. and Clemente, C. J. (2016). How to build your dragon: Scaling of muscle architecture from the world's smallest to the world's largest monitor lizard. *Front. Zool.* **13**, 1-17. doi:10.1186/s12983-016-0133-5

Dick, T. J. M. and Clemente, C. J. (2017). Where have all the giants gone? How animals deal with the problem of size. *PLoS Biol.* **15**, 1-10. doi:10.1371/journal.pbio.2000473

Eisenberg, B. R. (1983). Quantitative ultrastructure of mammalian skeletal muscle. In *Handbook of Physiology* (ed. L. Peachy and R. Adrian), pp. 73-112. American Physiological Society.

Eng, C. M., Smallwood, L. H., Rainiero, M. P., Lahey, M., Ward, S. R. and Lieber, R. L. (2008). Scaling of muscle architecture and fiber types in the rat hindlimb. *J. Exp. Biol.* **211**, 2336-2345. doi:10.1242/jeb.017640

Farmer, C. G. (2003). Reproduction: the adaptive significance of endothermy. *Am. Nat.* **162**, 826-840. doi:10.1086/380922

Farmer, C. G. (2020). Parental care, destabilizing selection, and the evolution of tetrapod endothermy. *Physiology* **35**, 160-176. doi:10.1152/physiol.00058.2018

Garland, T. (1984). Physiological correlates of locomotory performance in a lizard: an allometric approach. *Am. J. Physiol. Regul. Integr. Comp. Physiol.* **16**, 806-815. doi:10.1152/ajpregu.1984.247.5.R806

Garland, T. and Else, P. L. (1987). Seasonal, sexual, and individual variation in endurance and activity metabolism in lizards. *Am. J. Physiol.* **252**, R439-R449.

Gleeson, T. T. (1983). A histochemical and enzymatic study of the muscle fiber types in the water monitor, *Varanus salvator. J. Exp. Zool.* **227**, 191-201. doi:10.1002/jez.1402270204

Gleeson, T. T. and Harrison, J. M. (1986). Reptilian skeletal muscle: fiber-type composition and enzymatic profile in the lizard, *Iguana iguana. Copeia* **1986**, 324. doi:10.2307/1444993

Gleeson, T. T. and Harrison, J. M. (1988). Muscle composition and its relation to sprint running in the lizard *Dipsosaurus dorsalis. Am. J. Physiol. Regul. Integr. Comp. Physiol.* **255**, 470-477. doi:10.1152/ajpregu.1988.255.3.R470

Gleeson, T. T. and Johnston, I. A. (1987). Reptilian skeletal muscle: contractile properties of identified, single fast–twitch and slow fibers from the lizard *Dipsosaurus dorsalis. J. Exp. Zool.* **242**, 283-290. doi:10.1002/jez.1402420306

Gleeson, T. T., Putnam, R. W. and Bennett, A. F. (1980). Histochemical, enzymatic, and contractile properties of skeletal muscle fibers in the lizard *Dipsosaurus dorsalis. J. Exp. Zool.* **214**, 293-302. doi:10.1002/jez.1402140307

Hardy, K. M., Dillaman, R. M., Locke, B. R. and Kinsey, S. T. (2009). A skeletal muscle model of extreme hypertrophic growth reveals the influence of diffusion on cellular design. *Am. J. Physiol. Regul. Integr. Comp. Physiol.* **296**, 1855-1867. doi:10.1152/ajpregu.00076.2009

Hardy, K. M., Lema, S. C. and Kinsey, S. T. (2010). The metabolic demands of swimming behavior influence the evolution of skeletal muscle fiber design in the brachyuran crab family Portunidae. *Mar. Biol.* **157**, 221-236. doi:10.1007/s00227-009-1301-3

Hoppeler, H. and Flück, M. (2002). Normal mammalian skeletal muscle and its phenotypic plasticity. *J. Exp. Biol.* **205**, 2143-2152. doi:10.1242/jeb.205.15.2143

James, R. S., Vanhooydonck, B., Tallis, J. A. and Herrel, A. (2015). Larger lacertid lizard species produce higher than expected iliotibialis muscle power output: The evolution of muscle contractile mechanics with body size. *J. Exp. Biol.* **218**, 3589-3595. doi:10.1242/jeb.124974

Jayne, B. C., Bennett, A. F. and Lauder, G. V. (1990). Muscle recruitment during terrestrial locomotion: How speed and temperature affect fibre type use in a lizard. *J. Exp. Biol.* **152**, 101-128. doi:10.1242/jeb.152.1.101

Jimenez, A. G., Locke, B. R. and Kinsey, S. T. (2008). The influence of oxygen and high-energy phosphate diffusion on metabolic scaling in three species of tail-flipping crustaceans. *J. Exp. Biol.* **211**, 3214-3225. doi:10.1242/jeb.020677

Jimenez, A. G., Dasika, S. K., Locke, B. R. and Kinsey, S. T. (2011). An evaluation of muscle maintenance costs during fiber hypertrophy in the lobster *Homarus americanus*: Are larger muscle fibers cheaper to maintain? *J. Exp. Biol.* **214**, 3688-3697. doi:10.1242/jeb.060301

Jimenez, A. G., Dillaman, R. M. and Kinsey, S. T. (2013). Large fibre size in skeletal muscle is metabolically advantageous. *Nat. Commun.* **4**, 2150. doi:10.1038/ncomms3150

Johnston, I. A. (2006). Environment and plasticity of myogenesis in teleost fish. *J. Exp. Biol.* **209**, 2249-2264. doi:10.1242/jeb.02153

Johnston, I. A., Fernández, D. A., Calvo, J., Vieira, V. L. A., North, A. W., Abercromby, M. and Garland, T. (2003). Reduction in muscle fibre number during the adaptive radiation of notothenioid fishes: A phylogenetic perspective. *J. Exp. Biol.* **206**, 2595-2609. doi:10.1242/jeb.00474

Johnston, I. A., Abercromby, M., Vieira, V. L. A., Sigursteindóttir, R. J., Kristjánsson, B. K., Sibthorpe, D. and Skúlason, S. (2004). Rapid evolution of muscle fibre number in post-glacial populations of Arctic charr *Salvelinus alpinus. J. Exp. Biol.* **207**, 4343-4360. doi:10.1242/jeb.01292

Johnston, I. A., Abercromby, M. and Andersen, Ø. (2006). Muscle fibre number varies with haemoglobin phenotype in Atlantic cod as predicted by the optimal fibre number hypothesis. *Biol. Lett.* **2**, 590-592. doi:10.1098/rsbl.2006.0500

Johnston, I. A., Kristjánsson, B. K., Paxton, C. G. P., Vieira, V. L. A., Macqueen, D. J. and Bell, M. A. (2012). Universal scaling rules predict evolutionary patterns of myogenesis in species with indeterminate growth. *Proc. R. Soc. B Biol. Sci.* **279**, 2255-2261. doi:10.1098/rspb.2011.2536

Jorgenson, K. W., Phillips, S. M. and Hornberger, T. A. (2020). Identifying the structural adaptations that drive the mechanical load-induced growth of skeletal muscle: a scoping review. *Cells* **9**, 1658. doi:10.3390/cells9071658

Kielhorn, C. E., Dillaman, R. M., Kinsey, S. T., McLellan, W. A., Mark Gay, D., Dearolf, J. L. and Ann Pabst, D. (2013). Locomotor muscle profile of a deep (*Kogia breviceps*) versus shallow (*Tursiops truncatus*) diving cetacean. *J. Morphol.* **274**, 663-675. doi:10.1002/jmor.20124

Kinsey, S. T., Hardy, K. M. and Locke, B. R. (2007). The long and winding road: Influences of intracellular metabolite diffusion on cellular organization and metabolism in skeletal muscle. *J. Exp. Biol.* **210**, 3505-3512. doi:10.1242/jeb.000331

Kinsey, S. T., Locke, B. R. and Dillaman, R. M. (2011). Molecules in motion: Influences of diffusion on metabolic structure and function in skeletal muscle. *J. Exp. Biol.* **214**, 263-274. doi:10.1242/jeb.047985

Krivickas, L. S., Dorer, D. J., Ochala, J. and Frontera, W. R. (2011). Relationship between force and size in human single muscle fibres. *Exp. Physiol.* **96**, 539-547. doi:10.1113/expphysiol.2010.055269

Kroeger, J. P., McLellan, W. A., Arthur, L. H., Velten, B. P., Singleton, E. M., Kinsey, S. T. and Pabst, D. A. (2020). Locomotor muscle morphology of three species of pelagic delphinids. *J. Morphol.* **281**, 170-182. doi:10.1002/jmor.21089

Kumar, S., Stecher, G., Suleski, M. and Hedges, S. B. (2017). TimeTree: a resource for timelines, timetrees, and divergence times. *Moecular Biol. Evol.* **34**, 1812-1819. doi:10.1093/molbev/msx116

Leonard, K. C., Worden, N., Boettcher, M. L., Dickinson, E. and Hartstone-Rose, A. (2021a). Effects of freezing and short-term fixation on muscle mass, volume, and density. *Anat. Rec.* 1-10. doi:10.1002/ar.24639

Leonard, K. C., Worden, N., Boettcher, M. L., Dickinson, E. and Hartstone-Rose, A. (2021b). Effects of long-term ethanol storage on muscle architecture. *Anat. Rec.* 1-15. doi:10.1002/ar.24638

Marx, J. O., Olsson, M. C. and Larsson, L. (2006). Scaling of skeletal muscle shortening velocity in mammals representing a 100,000-fold difference in body size. *Pflugers Arch. Eur. J. Physiol.* **452**, 222-230. doi:10.1007/s00424-005-0017-6

Milligan, L. P. and McBride, B. W. (1985). Energy costs of ion pumping by animal tissues. *J. Nutr.* **115**, 1374-1382. doi:10.1093/jn/115.10.1374

Moyes, C. D. and Genge, C. E. (2010). Scaling of muscle metabolic enzymes: An historical perspective. *Comp. Biochem. Physiol. A Mol. Integr. Physiol.* **156**, 344-350. doi:10.1016/j.cbpa.2010.01.025

Pacifici, M., Santini, L., Di Marco, M., Baisero, D., Francucci, L., Marasini, G. G., Visconti, P. and Rondinini, C. (2013). Generation length for mammals. *Nat. Conserv.* **5**, 87-94. doi:10.3897/natureconservation.5.5734

Peter, J. B., Barnard, R. J. and Edgerton, V. R. (1972). Metabolic profiles of three fiber types of skeletal muscle in guinea pigs and rabbits. *Biochemistry* **11**, 2627-2633. doi:10.1021/bi00764a013

Priester, C., Morton, L. C., Kinsey, S. T., Watanabe, W. O. and Dillaman, R. M. (2011). Growth patterns and nuclear distribution in white muscle fibers from black sea bass, *Centropristis striata*: evidence for the influence of diffusion. *J. Exp. Biol.* **214**, 1230-1239. doi:10.1242/jeb.053199

Quintana, E., Manjarrez, J., Martínez-Gómez, M., D'Alba, L., Rodríguez-Antolín, J. and Fajardo, V. (2014). Sexual dimorphism in histological characteristics and contractility of the iliofibularis muscle in the lizard *Sceloporus torquatus*. *Acta Zool.* **95**, 264-271. doi:10.1111/azo.12021

Rehfeldt, C., Stickland, N., Fiedler, I. and Wegner, J. (1999). Environmental and genetic factors as sources of variation in skeletal muscle fibre number. *Basic Appl. Myol.* **9**, 235-254.

Rome, L. C. and Lindstedt, S. L. (1997). Mechanical and metabolic design of the muscular system in vertebrates. In *Handbook of Physiology: Comprehensive Physiology*, Vol. II (ed. W. Danttzler), pp. 1586-1651. Bethesda, MD: American Physiological Society.

Rome, L. C., Sosnicki, A. A. and Goble, D. O. (1990). Maximum velocity of shortening of three fibre types from horse soleus muscle: implications for scaling with body size. *J. Physiol.* **431**, 163-185. doi:10.1113/jphysiol.1990.sp018325

Scales, J. A., King, A. A. and Butler, M. A. (2009). Running for your life or running for your dinner: what drives fiber-type evolution in lizard locomotor muscles? *Am. Nat.* **173**, 543-553. doi:10.1086/597613

Schaart, G., Hesselink, R. P., Keizer, H. A., Van Kranenburg, G., Drost, M. R. and Hesselink, M. K. C. (2004). A modified PAS stain combined with immunofluorescence for quantitative analyses of glycogen in muscle sections. *Histochem. Cell Biol.* **122**, 161-169. doi:10.1007/s00418-004-0690-0

Schaeffer, P. J. and Lindstedt, S. L. (2013). How animals move: comparative lessons on animal locomotion. *Compr. Physiol.* **3**, 289-314. doi:10.1002/cphy.c110059

Schiaffino, S. and Reggiani, C. (2011). Fiber types in mammalian skeletal muscles. *Physiol. Rev.* **91**, 1447-1531. doi:10.1152/physrev.00031.2010

Seow, C. Y. and Ford, L. E. (1991). Shortening velocity and power output of skinned muscle fibers from mammals having a 25,000-fold range of body mass. *J. Gen. Physiol.* **97**, 541-560. doi:10.1085/jgp.97.3.541

Somero, G. N. and Childress, J. J. (1980). A violation of the metabolism-size scaling paradigm: activities of glycolytic enzymes in muscle increase in larger-size fish. *Physiol. Zool.* **53**, 322-337. doi:10.1086/physzool.53.3.30155794

Thomas, J. B., Brian, F., Stephanie, B. and Richard, L. L. (1994). Relationship between muscle fiber types and sizes and muscle architectural properties in the mouse hindlimb. *J. Morphol.* **221**, 177-190. doi:10.1002/jmor.1052210207

Thompson, G. G. (1996). Aspects of the morphology and metabolism of Western Australian goannas (Reptilia: Squamata: Varanidae) with particular reference to the effects of body mass and shape. PhD thesis, University of Western Australia School of Biological Sciences.

Thompson, G. G., Withers, P. C. and Cowan, E. (1997). Standard and maximal metabolic rates of goannas (Squamata: Varanidae). *Physiol. Zool.* **70**, 307-323. doi:10.1086/639605

Van Wessel, T., De Haan, A., Van Der Laarse, W. J. and Jaspers, R. T. (2010). The muscle fiber type-fiber size paradox: hypertrophy or oxidative metabolism? *Eur. J. Appl. Physiol.* **110**, 665-694. doi:10.1007/s00421-010-1545-0

Velten, B. P., Dillaman, R. M., Kinsey, S. T., McLellan, W. A. and Pabst, D. A. (2013). Novel locomotor muscle design in extreme deep-diving whales. *J. Exp. Biol.* **216**, 1862-1871. doi:10.1242/jeb.081323

Xu, J., Strasburg, G. M., Reed, K. M. and Velleman, S. G. (2021). Effect of temperature and selection for growth on intracellular lipid accumulation and adipogenic gene expression in Turkey pectoralis major muscle satellite cells. *Front. Physiol.* **12**, 1-16. doi:10.3389/fphys.2021.667814

Young, B. A., Magon, D. K. and Goslow, G. E. (1990). Length-tension and histochemical properties of select shoulder muscles of the savannah monitor lizard (*Varanus exanthematicus*): Implications for function and evolution. *J. Exp. Zool.* **256**, 63-74. doi:10.1002/jez.1402560109

Zurlo, F., Larson, K., Bogardus, C. and Ravussin, E. (1990). Skeletal muscle metabolism is a major determinant of resting energy expenditure. *J. Clin. Invest.* **86**, 1423-1427. doi:10.1172/JCI114857
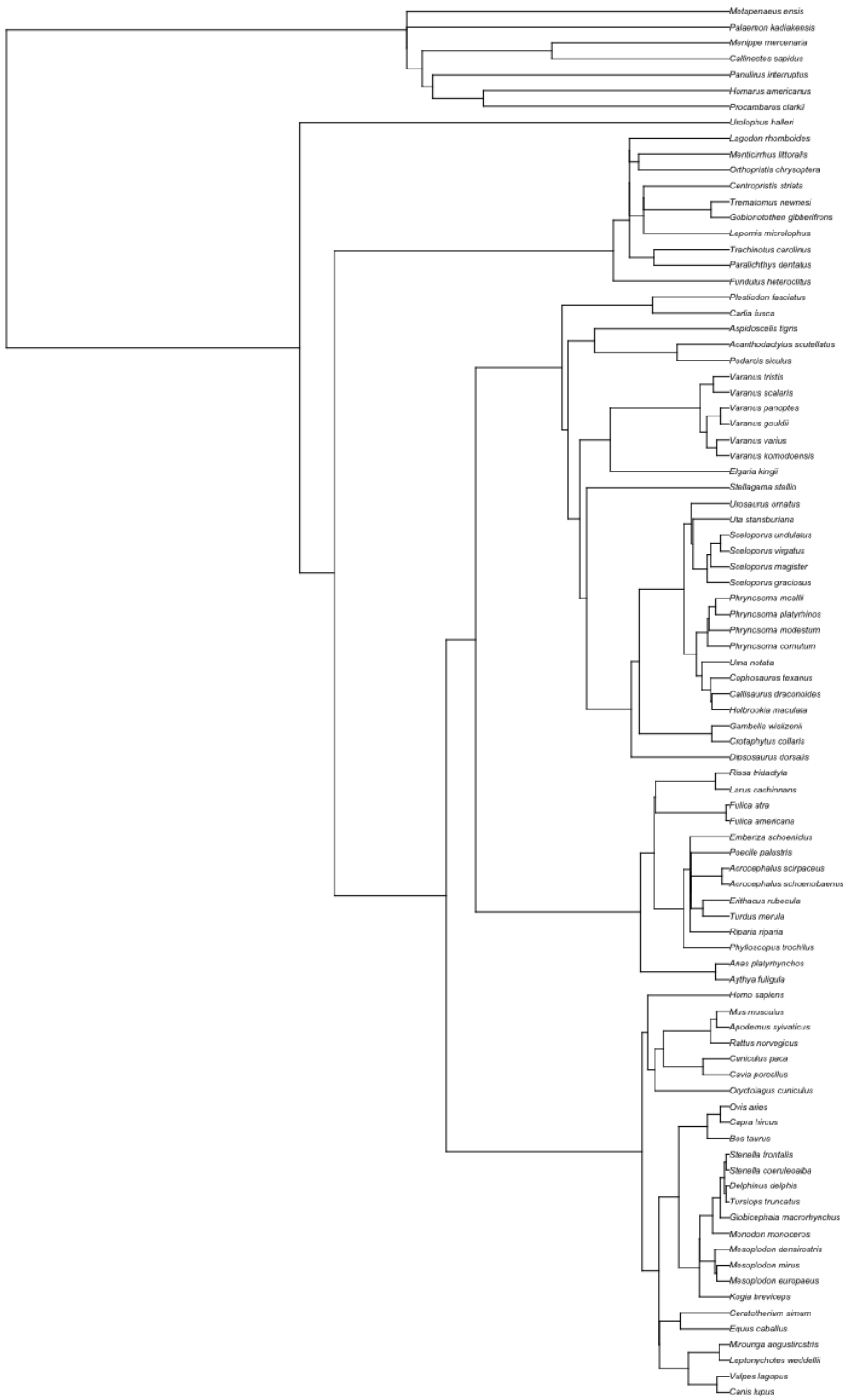
Fig. S1. Phylogenetic tree used in comparative analysis. Tree is also included as an .nwk file on figshare.

Table S1. Raw and mass-corrected mean fCSA values by muscle and individual

muscle	species	body mass (g)	Raw fCSA (μm^2)		Relative fCSA (μm^2)	
			mean	standard deviation	mean	standard deviation
cFem	*V. tristis*	104.5	6,499.66	1,268.43	62.20	12.14
cFem	*V. tristis*	163.3	7,644.47	592.60	46.81	3.63
cFem	*V. panoptes*	661.21	3,704.77	256.44	5.60	0.39
cFem	*V. varius*	810	3,211.71	236.96	3.97	0.29
cFem	*V. varius*	834	5,321.32	930.96	6.38	1.12
cFem	*V. panoptes*	997	5,544.28	533.40	5.56	0.54
cFem	*V. panoptes*	1,059.88	8,025.07	940.93	7.57	0.89
cFem	*V. varius*	4,025	7,265.99	322.96	1.81	0.08
cFem	*V. komodoensis*	30,000	24,778.66	11,534.93	0.83	0.38
cFem	*V. komodoensis*	40,000	7,591.19	1,125.02	0.19	0.03
femTib	*V. tristis*	104.5	7,876.51	1,123.09	75.37	10.75
femTib	*V. scalaris*	158.1	2,759.81	730.53	17.46	4.62
femTib	*V. tristis*	163.3	6,268.97	381.82	38.39	2.34
femTib	*V. varius*	810	4,528.49	485.82	5.59	0.60
femTib	*V. varius*	834	6,484.88	2,251.49	7.78	2.70
femTib	*V. panoptes*	997	11,555.49	372.60	11.59	0.37
femTib	*V. panoptes*	1,059.88	11,268.63	3,814.30	10.63	3.60
femTib	*V. varius*	4,025	15,961.82	7,148.07	3.97	1.78
femTib	*V. komodoensis*	30,000	30,188.29	-	1.01	0.00
femTib	*V. komodoensis*	40,000	18,462.98	1,085.76	0.46	0.03
FTIdeep	*V. tristis*	104.5	4,610.64	1,247.99	44.12	11.94
FTIdeep	*V. scalaris*	158.1	4,252.35	893.32	26.90	5.65
FTIdeep	*V. tristis*	163.3	6,318.58	865.71	38.69	5.30
FTIdeep	*V. varius*	810	5,669.94	--	7.00	--
FTIdeep	*V. varius*	834	3,781.07	--	4.53	--
FTIdeep	*V. panoptes*	997	8,581.47	1,646.59	8.61	1.65
FTIdeep	*V. panoptes*	1,059.88	8,682.06	1,355.53	8.19	1.28
FTIdeep	*V. varius*	4,025	11,426.89	--	2.84	--
FTIdeep	*V. komodoensis*	30,000	13,769.61	1,407.61	0.46	0.05
FTIdeep	*V. komodoensis*	40,000	5,269.33	678.24	0.13	0.02
FTIsup	*V. tristis*	104.5	4,814.96	650.50	46.08	6.22
FTIsup	*V. scalaris*	158.1	3,642.59	642.29	23.04	4.06
FTIsup	*V. tristis*	163.3	4,727.06	828.16	28.95	5.07
FTIsup	*V. varius*	810	3,954.12	--	4.88	--
FTIsup	*V. varius*	834	5,049.69	--	6.05	--
FTIsup	*V. panoptes*	997	4,335.67	963.97	4.35	0.97
FTIsup	*V. panoptes*	1,059.88	10,500.61	984.41	9.91	0.93
FTIsup	*V. varius*	4,025	15,451.04	--	3.84	--
FTIsup	*V. komodoensis*	30,000	12,413.70	--	0.41	--
FTIsup	*V. komodoensis*	40,000	16,182.82	--	0.40	--
gast	*V. tristis*	104.5	3,119.62	619.15	29.85	5.92
gast	*V. scalaris*	158.1	4,510.32	485.50	28.53	3.07
gast	*V. tristis*	163.3	3,677.10	--	22.52	--

gast	*V. gouldii*	429.4	5,847.88	347.21	13.62	0.81
gast	*V. gouldii*	439.8	3,380.39	405.86	7.69	0.92
gast	*V. gouldii*	459.3	3,506.02	640.20	7.63	1.39
gast	*V. panoptes*	661.21	4,173.04	1,560.35	6.31	2.36
gast	*V. varius*	810	3,223.55	261.86	3.98	0.32
gast	*V. varius*	834	5,198.79	549.71	6.23	0.66
gast	*V. panoptes*	997	3,362.91	469.49	3.37	0.47
gast	*V. panoptes*	1,059.88	8,420.07	1,718.24	7.94	1.62
gast	*V. panoptes*	2,076.8	15,998.01	5,128.63	7.70	2.47
gast	*V. varius*	4,025	16,294.56	2,001.01	4.05	0.50
gast	*V. komodoensis*	30,000	14,453.57	1,566.63	0.48	0.05
gast	*V. komodoensis*	40,000	8,577.71	--	0.21	--
ilFem	*V. tristis*	104.5	2,071.16	623.90	19.82	5.97
ilFem	*V. scalaris*	158.1	2,948.93	296.70	18.65	1.88
ilFem	*V. tristis*	163.3	6,930.08	953.42	42.44	5.84
ilFem	*V. varius*	810	6,061.00	--	7.48	--
ilFem	*V. varius*	834	9,249.29	--	11.09	--
ilFem	*V. panoptes*	997	3,996.54	1,225.36	4.01	1.23
ilFem	*V. panoptes*	1,059.88	4,467.86	187.87	4.22	0.18
ilFem	*V. varius*	4,025	8,949.86	--	2.22	--
ilFem	*V. komodoensis*	30,000	7,529.79	1,426.54	0.25	0.05
ilFem	*V. komodoensis*	40,000	6,306.21	1,620.95	0.16	0.04
ilFib	*V. tristis*	104.5	5,104.01	1,319.41	48.84	12.63
ilFib	*V. scalaris*	158.1	3,426.04	1,141.04	21.67	7.22
ilFib	*V. tristis*	163.3	4,434.15	301.24	27.15	1.84
ilFib	*V. gouldii*	429.4	7,233.26	1,984.78	16.85	4.62
ilFib	*V. gouldii*	439.8	4,596.89	1,180.49	10.45	2.68
ilFib	*V. gouldii*	459.3	5,906.07	2,297.15	12.86	5.00
ilFib	*V. panoptes*	661.21	2,879.90	1,561.23	4.36	2.36
ilFib	*V. varius*	810	4,461.53	970.24	5.51	1.20
ilFib	*V. varius*	834	4,472.49	1,199.65	5.36	1.44
ilFib	*V. panoptes*	997	4,722.56	1,228.43	4.74	1.23
ilFib	*V. panoptes*	1,059.88	5,784.59	1,419.43	5.46	1.34
ilFib	*V. panoptes*	2,076.8	5,560.71	2,743.61	2.68	1.32
ilFib	*V. varius*	4,025	8,114.42	881.47	2.02	0.22
ilFib	*V. komodoensis*	30,000	15,618.95	6,942.74	0.52	0.23
ilFib	*V. komodoensis*	40,000	8,961.49	1,562.80	0.24	0.07
ilTib	*V. tristis*	104.5	7,297.89	2,548.92	69.84	24.39
ilTib	*V. scalaris*	158.1	2,910.14	352.97	18.41	2.23
ilTib	*V. tristis*	163.3	3,980.88	1,113.23	24.38	6.82
ilTib	*V. gouldii*	439.8	5,188.40	546.12	11.80	1.24
ilTib	*V. gouldii*	459.3	3,419.67	1,937.69	7.45	4.22
ilTib	*V. panoptes*	661.21	3,853.98	131.42	5.83	0.20
ilTib	*V. varius*	834	4,284.02	414.84	5.14	0.50
ilTib	*V. panoptes*	997	6,174.24	1,085.81	6.19	1.09
ilTib	*V. panoptes*	1,059.88	5,037.14	530.38	4.75	0.50
ilTib	*V. panoptes*	2,076.8	2,560.57	668.75	1.23	0.32
ilTib	*V. varius*	4,025	12,271.05	970.96	3.05	0.24

ilTib	*V. komodoensis*	30,000	11,352.46	6,338.59	0.38	0.21
ilTib	*V. komodoensis*	40,000	8,201.48	1,944.28	0.21	0.05
pLong	*V. tristis*	104.5	5,660.09	2,299.33	54.16	22.00
pLong	*V. scalaris*	158.1	3,650.03	617.71	23.09	3.91
pLong	*V. tristis*	163.3	2,888.58	353.85	17.69	2.17
pLong	*V. panoptes*	661.21	2,650.28	328.44	4.01	0.50
pLong	*V. varius*	810	2,983.45	298.23	3.68	0.37
pLong	*V. varius*	834	4,097.80	523.69	4.91	0.63
pLong	*V. panoptes*	997	4,244.36	488.77	4.26	0.49
pLong	*V. panoptes*	1,059.88	5,935.56	1,078.07	5.60	1.02
pLong	*V. varius*	4,025	16,113.57	2,549.59	4.00	0.63
pLong	*V. komodoensis*	30,000	12,716.55	4,041.46	0.42	0.13
pLong	*V. komodoensis*	40,000	12,664.75	2,731.63	0.32	0.07
pTib	*V. tristis*	104.5	5,988.35	352.70	57.30	3.38
pTib	*V. scalaris*	158.1	3,650.03	617.71	23.09	3.91
pTib	*V. panoptes*	661.21	2,650.28	328.44	4.01	0.50
pTib	*V. varius*	810	3,945.06	522.01	4.87	0.64
pTib	*V. varius*	834	5,728.34	2,034.81	6.87	2.44
pTib	*V. panoptes*	997	3,958.92	655.38	3.97	0.66
pTib	*V. panoptes*	1,059.88	7,375.38	624.64	6.96	0.59
pTib	*V. varius*	4,025	13,453.17	1,527.09	3.34	0.38
pTib	*V. komodoensis*	30,000	6,359.45	2,640.52	0.21	0.09
pTib	*V. komodoensis*	40,000	14,515.04	4,247.53	0.36	0.11
tibAnt	*V. tristis*	104.5	2,278.34	322.44	21.80	3.09
tibAnt	*V. scalaris*	158.1	3,465.21	910.04	21.92	5.76
tibAnt	*V. tristis*	163.3	2,577.09	473.29	15.78	2.90
tibAnt	*V. gouldii*	429.4	4,578.79	1,352.71	10.66	3.15
tibAnt	*V. gouldii*	439.8	3,308.69	894.38	7.52	2.03
tibAnt	*V. gouldii*	459.3	4,037.06	419.28	8.79	0.91
tibAnt	*V. panoptes*	661.21	2,571.31	67.01	3.89	0.10
tibAnt	*V. varius*	810	2,972.41	376.24	3.67	0.46
tibAnt	*V. varius*	834	2,939.13	255.49	3.52	0.31
tibAnt	*V. panoptes*	997	3,506.42	1,850.42	3.52	1.86
tibAnt	*V. panoptes*	1,059.88	4,629.20	1,084.05	4.37	1.02
tibAnt	*V. panoptes*	2,076.8	2,914.57	1,003.90	1.40	0.48
tibAnt	*V. varius*	4,025	7,953.19	821.88	1.98	0.20
tibAnt	*V. komodoensis*	30,000	9,488.02	2,771.43	0.32	0.09
tibAnt	*V. komodoensis*	40,000	9,386.37	2,359.34	0.23	0.06